Liquid-gas phase transition in the canonical ensemble of asymmetric nuclear matter

K. Miyazaki

E-mail: miyazakiro@rio.odn.ne.jp

Abstract

New calculus of the liquid-gas phase transition is developed for the canonical ensemble of asymmetric nuclear matter. In contrast to the familiar geometrical construction, the pressure and the chemical potentials are determined for definite values of the baryon densities of proton and neutron and the temperature. Because the derivatives of chemical potentials by pressure have discontinuities at the ends of the phase transition, we conclude against the preceding works that the phase transition is the first order. Due to the field-dependent meson-nucleon coupling constants in our relativistic mean-field model of nuclear matter, the section of binodal surface has no critical point. The appearance of the retrograde condensation is also proved.

The liquid-gas phase transition in warm nuclear matter [1,2] is a recent topic in nuclear physics. It is experimentally investigated [3,4] in the multifragmentation reactions of heavy ions. The nuclear matter produced in the reaction is charge asymmetric. It is a binary system that has two independent chemical potentials of proton and neutron. Based on the Gibbs condition in the phase equilibrium, both the chemical potentials in gaseous and liquid phases are equilibrated. Reference [5] determined them in terms of the geometrical construction, which was also used in the other works [6-9] of the liquid-gas phase transition in asymmetric nuclear matter.

In the geometrical construction, the chemical potentials are determined for a fixed value of the pressure and the asymmetry of nuclear matter. However, the object is neither a canonical nor a grand-canonical ensemble. In contrast to the condensed matter physics we cannot press nuclear matter under a definite pressure in nuclear experiments. In this point of view, the geometrical construction is not physically consistent with the liquid-gas phase transition in nuclear multifragmentation reactions. On the other hand, another strategy is proposed recently in Ref. [10], which considers a neutron grand-canonical but proton canonical ensemble. The investigation of phase equilibrium is much easier than the geometrical construction because the Maxwell construction is applicable. Nevertheless, the total system in Ref. [10] is neither canonical nor grand-canonical yet.

In the present paper we investigate for the first time the liquid-gas phase transition in the canonical ensemble of binary nuclear system. We are based on the relativistic mean-field (RMF) model of asymmetric nuclear matter developed in Refs. [11] and [12]. The

model has advantages over the other RMF models in Refs. [5-8]. It can reproduce the recent astronomical observations of NSs, the density-dependence of the nuclear symmetry energy and the critical temperature of symmetric nuclear matter. The successes are essentially due to the field-dependent effective NNX ($X = \sigma$, ω, δ and ρ) coupling constants in the model:

$$g^*_{pp(nn)X} = \frac{1}{2}\left[(1+\lambda_X) + (1-\lambda_X)\left(\left(m^*_{p(n)}\right)^2 - v^2_{p(n)}\right)\right] g_{NNX}, \tag{1}$$

where $M^*_i = m^*_i M_N$ is the effective mass and $V_i = v_i M_N$ is the vector potential of a proton or a neutron in the medium. We assume $\lambda_\sigma = \lambda_\omega = 2/3$ and $\lambda_\delta = \lambda_\rho = 0$. The coupling constants g_{NNX} are determined in Ref. [11].

At finite temperature T the thermodynamic potential per volume $\tilde{\Omega} \equiv \Omega/V$ is

$$\begin{aligned}\tilde{\Omega} &= \frac{1}{2} m_\sigma^2 \langle\sigma\rangle^2 + \frac{1}{2} m_\delta^2 \langle\delta_3\rangle^2 - \frac{1}{2} m_\omega^2 \langle\omega_0\rangle^2 - \frac{1}{2} m_\rho^2 \langle\rho_{03}\rangle^2 \\ &- \gamma\, k_B\, T \sum_{i=p,n} \int_0^\infty \frac{d^3\mathbf{k}}{(2\pi)^3} \left\{ \ln\left[1 + \exp\left(\frac{\nu_i - E^*_{ki}}{k_B\, T}\right)\right] + \ln\left[1 + \exp\left(\frac{-\nu_i - E^*_{ki}}{k_B\, T}\right)\right]\right\},\end{aligned} \tag{2}$$

where k_B is the Boltzmann constant and $E^*_{ki} = (\mathbf{k}^2 + M^{*2}_i)^{1/2}$. The spin-isospin degeneracy is $\gamma = 2$. The ν_i is defined using the chemical potential μ_i and the vector potential V_i of a proton or a neutron as

$$\nu_i = \mu_i - V_i. \tag{3}$$

The effective masses and the vector potentials are determined by extremizing $\tilde{\Omega}$:

$$\begin{aligned}\frac{\partial\,\tilde{\Omega}}{\partial M^*_p} &= \rho_{Sp} + m_\sigma^2 \frac{\langle\sigma\rangle}{M_N} \frac{\partial\,\langle\sigma\rangle}{\partial\, m^*_p} + m_\delta^2 \frac{\langle\delta_3\rangle}{M_N} \frac{\partial\,\langle\delta_3\rangle}{\partial\, m^*_p} \\ &- m_\omega^2 \frac{\langle\omega_0\rangle}{M_N} \frac{\partial\,\langle\omega_0\rangle}{\partial\, m^*_p} - m_\rho^2 \frac{\langle\rho_{03}\rangle}{M_N} \frac{\partial\,\langle\rho_{03}\rangle}{\partial\, m^*_p} = 0,\end{aligned} \tag{4}$$

$$\begin{aligned}\frac{\partial\,\tilde{\Omega}}{\partial\, V_p} &= \rho_{Bp} + m_\sigma^2 \frac{\langle\sigma\rangle}{M_N} \frac{\partial\,\langle\sigma\rangle}{\partial\, v_p} + m_\delta^2 \frac{\langle\delta_3\rangle}{M_N} \frac{\partial\,\langle\delta_3\rangle}{\partial\, v_p} \\ &- m_\omega^2 \frac{\langle\omega_0\rangle}{M_N} \frac{\partial\,\langle\omega_0\rangle}{\partial\, v_p} - m_\rho^2 \frac{\langle\rho_{03}\rangle}{M_N} \frac{\partial\,\langle\rho_{03}\rangle}{\partial\, v_p} = 0,\end{aligned} \tag{5}$$

$$\begin{aligned}\frac{\partial\,\tilde{\Omega}}{\partial M^*_n} &= \rho_{Sn} + m_\sigma^2 \frac{\langle\sigma\rangle}{M_N} \frac{\partial\,\langle\sigma\rangle}{\partial\, m^*_n} + m_\delta^2 \frac{\langle\delta_3\rangle}{M_N} \frac{\partial\,\langle\delta_3\rangle}{\partial\, m^*_n} \\ &- m_\omega^2 \frac{\langle\omega_0\rangle}{M_N} \frac{\partial\,\langle\omega_0\rangle}{\partial\, m^*_n} - m_\rho^2 \frac{\langle\rho_{03}\rangle}{M_N} \frac{\partial\,\langle\rho_{03}\rangle}{\partial\, m^*_n} = 0,\end{aligned} \tag{6}$$

$$\frac{\partial\,\tilde{\Omega}}{\partial\,V_n} = \rho_{Bn} + m_\sigma^2\,\frac{\langle\sigma\rangle}{M_N}\,\frac{\partial\,\langle\sigma\rangle}{\partial\,v_n} + m_\delta^2\,\frac{\langle\delta_3\rangle}{M_N}\,\frac{\partial\,\langle\delta_3\rangle}{\partial\,v_n} - m_\omega^2\,\frac{\langle\omega_0\rangle}{M_N}\,\frac{\partial\,\langle\omega_0\rangle}{\partial\,v_n} - m_\rho^2\,\frac{\langle\rho_{03}\rangle}{M_N}\,\frac{\partial\,\langle\rho_{03}\rangle}{\partial\,v_n} \;=\; 0, \tag{7}$$

where the mean-fields are calculated [11] from the effective masses and the vector potentials. The explicit expressions of the derivatives of mean fields are also given in Ref. [11]. The baryon and scalar densities are defined by

$$\rho_{Bi} = \gamma \int_0^\infty \frac{d^3\mathbf{k}}{(2\pi)^3}\,[\,n_{ki}\,(m_i^*, v_i, \mu_i\,; T) - \bar{n}_{ki}\,(m_i^*, v_i, \mu_i\,; T)], \tag{8}$$

$$\rho_{Si} = \gamma \int_0^\infty \frac{d^3\mathbf{k}}{(2\pi)^3}\,\frac{M_i^*}{E_{ki}^*}\,[\,n_{ki}\,(m_i^*, v_i, \mu_i\,; T) + \bar{n}_{ki}\,(m_i^*, v_i, \mu_i\,; T)]. \tag{9}$$

The Fermi-Dirac distribution functions of nucleon and antinucleon are

$$n_{ki}\,(m_i^*, v_i, \mu_i\,; T) = \left[\,1 + \exp\left(\frac{E_{ki}^* - \nu_i}{k_B\,T}\right)\right]^{-1}, \tag{10}$$

$$\bar{n}_{ki}\,(m_i^*, v_i, \mu_i\,; T) = \left[\,1 + \exp\left(\frac{E_{ki}^* + \nu_i}{k_B\,T}\right)\right]^{-1}. \tag{11}$$

In the following numerical analyses we have performed the Fermi integral directly using the adaptive automatic integration with 20-points Gaussian quadrature.

As mentioned above we consider the canonical ensemble of asymmetric nuclear matter. In other words we specify the temperature T and the baryon densities of proton and neutron in nuclear matter. In place of each baryon density the total baryon density

$$\rho_B = \rho_{Bp} + \rho_{Bn}, \tag{12}$$

and the isospin asymmetry

$$a = \frac{\rho_{Bn} - \rho_{Bp}}{\rho_B}, \tag{13}$$

are specified. Then, the 6th-rank nonlinear simultaneous equations (4)-(7), (12) and (13) are solved so that we have the effective masses, the vector potentials and the chemical potentials of proton and neutron. Using the results, the pressure is calculated by

$$P \;=\; \frac{1}{3\pi^2}\sum_{i=p,n}\int_0^\infty dk\,\frac{k^4}{E_{ki}^*}\,[\,n_{ki}\,(m_i^*, v_i, \mu_i\,; T) + \bar{n}_{ki}\,(m_i^*, v_i, \mu_i\,; T)] - \frac{1}{2}\,m_\sigma^2\,\langle\sigma\rangle^2 - \frac{1}{2}\,m_\delta^2\,\langle\delta_3\rangle^2 + \frac{1}{2}\,m_\omega^2\,\langle\omega_0\rangle^2 + \frac{1}{2}\,m_\rho^2\,\langle\rho_{03}\rangle^2\,. \tag{14}$$

The black curve in Fig. 1 shows an isotherm in the pressure-density plane for $a = 0.3$ and $T = 13$MeV. (We set the Boltzmann constant as unit.) It exhibits typical nature of van der Waals equation-of-state. The black curve in Fig. 2 shows the Helmholtz energy per baryon $F/A = G/A - P/\rho_B$ as a function of volume, where $G/A = \big(\mu_p\rho_{Bp} + \mu_n\rho_{Bn}\big)/\rho_B$ is the Gibbs energy per baryon. A concave on the curve is a signal of the liquid-gas phase transition. Because the physical Helmholtz energy must be convex, we can draw the common tangent depicted by the red line between $\rho_B^{-1} = 9.64\text{fm}^3$ and 47.54fm^3 marked by the red dots. Its inclination is the pressure $P = 0.165\text{MeV/fm}^3$ in the phase transition, which is shown by the red horizontal line in Fig. 1. The pressure is also determined from a crossing point on the black curve in Fig. 3, which shows the Gibbs energy per baryon as a function of pressure. The Gibbs energy on the crossing point is its equilibrated value in gaseous and liquid phases. To the contrary, the chemical potentials μ_p and μ_n are not equilibrated. As a matter of fact the black solid curves in Figs. 4 and 5, which show the chemical potentials as the functions of pressure, have discontinuities denoted by the vertical red dashed lines. We have $\mu_p = 909.5$MeV and $\mu_n = 923.5$MeV in gaseous phase but $\mu_p = 898.7$MeV and $\mu_n = 929.3$MeV in liquid phase. The black dashed curves correspond to the concave of the Helmholtz energy in Fig. 2 and so are not physically realized. Consequently, the Gibbs condition on the phase equilibrium is not satisfied.

So as to construct the physically reasonable liquid-gas mixed phase to be consistent with the Gibbs condition, we have to calculate the following 11th-rank simultaneous nonlinear equations. The four equations of them determine the effective masses and the vector potentials of proton and neutron in gaseous phase:

$$\begin{aligned}\frac{\partial\,\tilde{\Omega}}{\partial M_p^{(g)*}} &= \rho_{Sp}^{(g)} + m_\sigma^2\,\frac{\langle\sigma\rangle_g}{M_N}\,\frac{\partial\,\langle\sigma\rangle_g}{\partial\,m_p^{(g)*}} + m_\delta^2\,\frac{\langle\delta_3\rangle_g}{M_N}\,\frac{\partial\,\langle\delta_3\rangle_g}{\partial\,m_p^{(g)*}} \\ &\quad - m_\omega^2\,\frac{\langle\omega_0\rangle_g}{M_N}\,\frac{\partial\,\langle\omega_0\rangle_g}{\partial\,m_p^{(g)*}} - m_\rho^2\,\frac{\langle\rho_{03}\rangle_g}{M_N}\,\frac{\partial\,\langle\rho_{03}\rangle_g}{\partial\,m_p^{(g)*}} \;=\; 0, \end{aligned} \tag{15}$$

$$\begin{aligned}\frac{\partial\,\tilde{\Omega}}{\partial\,V_p^{(g)}} &= \rho_{Bp}^{(g)} + m_\sigma^2\,\frac{\langle\sigma\rangle_g}{M_N}\,\frac{\partial\,\langle\sigma\rangle_g}{\partial\,v_p^{(g)}} + m_\delta^2\,\frac{\langle\delta_3\rangle_g}{M_N}\,\frac{\partial\,\langle\delta_3\rangle_g}{\partial\,v_p^{(g)}} \\ &\quad - m_\omega^2\,\frac{\langle\omega_0\rangle_g}{M_N}\,\frac{\partial\,\langle\omega_0\rangle_g}{\partial\,v_p^{(g)}} - m_\rho^2\,\frac{\langle\rho_{03}\rangle_g}{M_N}\,\frac{\partial\,\langle\rho_{03}\rangle_g}{\partial\,v_p^{(g)}} \;=\; 0, \end{aligned} \tag{16}$$

$$\begin{aligned}\frac{\partial\,\tilde{\Omega}}{\partial M_n^{(g)*}} &= \rho_{Sn}^{(g)} + m_\sigma^2\,\frac{\langle\sigma\rangle_g}{M_N}\,\frac{\partial\,\langle\sigma\rangle_g}{\partial\,m_n^{(g)*}} + m_\delta^2\,\frac{\langle\delta_3\rangle_g}{M_N}\,\frac{\partial\,\langle\delta_3\rangle_g}{\partial\,m_n^{(g)*}} \\ &\quad - m_\omega^2\,\frac{\langle\omega_0\rangle_g}{M_N}\,\frac{\partial\,\langle\omega_0\rangle_g}{\partial\,m_n^{(g)*}} - m_\rho^2\,\frac{\langle\rho_{03}\rangle_g}{M_N}\,\frac{\partial\,\langle\rho_{03}\rangle_g}{\partial\,m_n^{(g)*}} \;=\; 0, \end{aligned} \tag{17}$$

$$\frac{\partial\,\tilde{\Omega}}{\partial\,V_n^{(g)}} = \rho_{Bn}^{(g)} + m_\sigma^2\,\frac{\langle\sigma\rangle_g}{M_N}\,\frac{\partial\,\langle\sigma\rangle_g}{\partial\,v_n^{(g)}} + m_\delta^2\,\frac{\langle\delta_3\rangle_g}{M_N}\,\frac{\partial\,\langle\delta_3\rangle_g}{\partial\,v_n^{(g)}} - m_\omega^2\,\frac{\langle\omega_0\rangle_g}{M_N}\,\frac{\partial\,\langle\omega_0\rangle_g}{\partial\,v_n^{(g)}} - m_\rho^2\,\frac{\langle\rho_{03}\rangle_g}{M_N}\,\frac{\partial\,\langle\rho_{03}\rangle_g}{\partial\,v_n^{(g)}} = 0, \tag{18}$$

where the suffix g indicates the gaseous phase. It is noted again that the mean-fields are expressed by the effective masses and the vector potentials. Similarly, the equations for liquid phase are

$$\frac{\partial\,\tilde{\Omega}}{\partial M_p^{(l)*}} = \rho_{Sp}^{(l)} + m_\sigma^2\,\frac{\langle\sigma\rangle_l}{M_N}\,\frac{\partial\,\langle\sigma\rangle_l}{\partial\,m_p^{(l)*}} + m_\delta^2\,\frac{\langle\delta_3\rangle_l}{M_N}\,\frac{\partial\,\langle\delta_3\rangle_l}{\partial\,m_p^{(l)*}} - m_\omega^2\,\frac{\langle\omega_0\rangle_l}{M_N}\,\frac{\partial\,\langle\omega_0\rangle_l}{\partial\,m_p^{(l)*}} - m_\rho^2\,\frac{\langle\rho_{03}\rangle_l}{M_N}\,\frac{\partial\,\langle\rho_{03}\rangle_l}{\partial\,m_p^{(l)*}} = 0, \tag{19}$$

$$\frac{\partial\,\tilde{\Omega}}{\partial\,V_p^{(l)}} = \rho_{Bp}^{(l)} + m_\sigma^2\,\frac{\langle\sigma\rangle_l}{M_N}\,\frac{\partial\,\langle\sigma\rangle_l}{\partial\,v_p^{(l)}} + m_\delta^2\,\frac{\langle\delta_3\rangle_l}{M_N}\,\frac{\partial\,\langle\delta_3\rangle_l}{\partial\,v_p^{(l)}} - m_\omega^2\,\frac{\langle\omega_0\rangle_l}{M_N}\,\frac{\partial\,\langle\omega_0\rangle_l}{\partial\,v_p^{(l)}} - m_\rho^2\,\frac{\langle\rho_{03}\rangle_l}{M_N}\,\frac{\partial\,\langle\rho_{03}\rangle_l}{\partial\,v_p^{(l)}} = 0, \tag{20}$$

$$\frac{\partial\,\tilde{\Omega}}{\partial M_n^{(l)*}} = \rho_{Sn}^{(l)} + m_\sigma^2\,\frac{\langle\sigma\rangle_l}{M_N}\,\frac{\partial\,\langle\sigma\rangle_l}{\partial\,m_n^{(l)*}} + m_\delta^2\,\frac{\langle\delta_3\rangle_l}{M_N}\,\frac{\partial\,\langle\delta_3\rangle_l}{\partial\,m_n^{(l)*}} - m_\omega^2\,\frac{\langle\omega_0\rangle_l}{M_N}\,\frac{\partial\,\langle\omega_0\rangle_l}{\partial\,m_n^{(l)*}} - m_\rho^2\,\frac{\langle\rho_{03}\rangle_l}{M_N}\,\frac{\partial\,\langle\rho_{03}\rangle_l}{\partial\,m_n^{(l)*}} = 0, \tag{21}$$

$$\frac{\partial\,\tilde{\Omega}}{\partial\,V_n^{(l)}} = \rho_{Bn}^{(l)} + m_\sigma^2\,\frac{\langle\sigma\rangle_l}{M_N}\,\frac{\partial\,\langle\sigma\rangle_l}{\partial\,v_n^{(l)}} + m_\delta^2\,\frac{\langle\delta_3\rangle_l}{M_N}\,\frac{\partial\,\langle\delta_3\rangle_l}{\partial\,v_n^{(l)}} - m_\omega^2\,\frac{\langle\omega_0\rangle_l}{M_N}\,\frac{\partial\,\langle\omega_0\rangle_l}{\partial\,v_n^{(l)}} - m_\rho^2\,\frac{\langle\rho_{03}\rangle_l}{M_N}\,\frac{\partial\,\langle\rho_{03}\rangle_l}{\partial\,v_n^{(l)}} = 0. \tag{22}$$

The other two equations determine the mixture of gas and liquid in the phase transition:

$$\rho_{Bp} = \frac{1}{2}\,(1-a)\,\rho_B = f_g\,\rho_{Bp}^{(g)} + (1-f_g)\,\rho_{Bp}^{(l)}, \tag{23}$$

$$\rho_{Bn} = \frac{1}{2}\,(1+a)\,\rho_B = f_g\,\rho_{Bn}^{(g)} + (1-f_g)\,\rho_{Bn}^{(l)}, \tag{24}$$

where f_g $(0 \le f_g \le 1)$ is the ratio of gas. The baryon densities in gaseous and liquid phases are

$$\rho_{Bi}^{(g)} = \gamma \int_0^\infty \frac{d^3\mathbf{k}}{(2\pi)^3}\left[\,n_{ki}\left(m_i^{(g)*}, v_i^{(g)}, \mu_i\,; T\right) - \bar{n}_{ki}\left(m_i^{(g)*}, v_i^{(g)}, \mu_i\,; T\right)\right], \tag{25}$$

$$\rho_{Bi}^{(l)} = \gamma \int_0^\infty \frac{d^3\mathbf{k}}{(2\pi)^3} \left[n_{ki}\left(m_i^{(l)*}, v_i^{(l)}, \mu_i\,; T\right) - \bar{n}_{ki}\left(m_i^{(l)*}, v_i^{(l)}, \mu_i\,; T\right)\right]. \tag{26}$$

The last equation imposes the equilibrium condition on pressures in gaseous and liquid phases:

$$\begin{aligned}
&\frac{1}{3\pi^2}\sum_{i=p,n}\int_0^\infty dk\,\frac{k^4}{E_{ki}^*}\left[n_{ki}\left(m_i^{(g)*}, v_i^{(g)}, \mu_i\,; T\right) + \bar{n}_{ki}\left(m_i^{(g)*}, v_i^{(g)}, \mu_i\,; T\right)\right] \\
&\qquad - \frac{1}{2}m_\sigma^2\langle\sigma\rangle_g^2 - \frac{1}{2}m_\delta^2\langle\delta_3\rangle_g^2 + \frac{1}{2}m_\omega^2\langle\omega_0\rangle_g^2 + \frac{1}{2}m_\rho^2\langle\rho_{03}\rangle_g^2 \\
&= \frac{1}{3\pi^2}\sum_{i=p,n}\int_0^\infty dk\,\frac{k^4}{E_{ki}^*}\left[n_{ki}\left(m_i^{(l)*}, v_i^{(l)}, \mu_i\,; T\right) + \bar{n}_{ki}\left(m_i^{(l)*}, v_i^{(l)}, \mu_i\,; T\right)\right] \\
&\qquad - \frac{1}{2}m_\sigma^2\langle\sigma\rangle_l^2 - \frac{1}{2}m_\delta^2\langle\delta_3\rangle_l^2 + \frac{1}{2}m_\omega^2\langle\omega_0\rangle_l^2 + \frac{1}{2}m_\rho^2\langle\rho_{03}\rangle_l^2\,.
\end{aligned} \tag{27}$$

Solving Eqs. (15)-(24) and (27), we have the effective masses and the vector potentials of proton and neutron in each of phases, the chemical potentials of proton and neutron, and the ratio of gas (or liquid) in the phase transition. It is noted again that in the canonical ensemble the chemical potentials μ_p and μ_n are determined for the definite baryon densities (23) and (24). For numerical calculations we have used the globally convergent Newton algorism in Ref. [13]. The trial values are easily found from the corresponding results in the common tangent method.

The numerical results for $a = 0.3$ and $T = 13$MeV are shown by the blue curves in Figs. 1-5. In Fig. 1 the pressure, which is the value of the right or left hand side of Eq. (27), increases slowly in the phase transition from gas to liquid against the constant pressure from the common tangent. The region of phase transition between $\rho_B = 0.017\text{fm}^{-3}$ and 0.109fm^{-3} is wider than the one between $\rho_B = 0.021\text{fm}^{-3}$ and 0.104fm^{-3} from the common tangent. This is due to the fact that the Helmholtz energy in Fig. 2 is convex and minimized so as to be lower than the common tangent. It is noted that the minimization of the Helmholtz energy leads to the equilibrium condition on pressure and chemical potentials in the isothermal process through the fundamental thermodynamic equation $dF = -SdT - PdV + \sum_{i=p,n}\mu_i dN_i$. The Gibbs energy in Fig. 3 is also minimized as a function of pressure because of $G/A = F/A + P/\rho_B$. The chemical potentials in Figs. 4 and 5 become the continuous functions of pressure. Figure 6 shows the ratio of liquid $f_l = 1 - f_g$, the asymmetry of gas $a_g = \frac{\left(\rho_{Bn}^{(g)} - \rho_{Bp}^{(g)}\right)}{\left(\rho_{Bn}^{(g)} + \rho_{Bp}^{(g)}\right)}$ and the asymmetry of liquid $a_l = \frac{\left(\rho_{Bn}^{(l)} - \rho_{Bp}^{(l)}\right)}{\left(\rho_{Bn}^{(l)} + \rho_{Bp}^{(l)}\right)}$ in the phase transition.

Here we have to discuss the order of the phase transition. Because the black curve and the blue dashed curve in Fig. 3 connect smoothly on the points marked by the blue dots,

$\partial G/\partial P$ has no discontinuity. Reference [5] therefore asserts that the liquid-gas phase transition in asymmetric nuclear matter is the second order. However, the argument is not consistent with the Gibbs condition, to which each of the chemical potentials rather than the Gibbs energy is relevant. We see readily in Figs. 4 and 5 that $\partial\mu_p/\partial P$ and $\partial\mu_n/\partial P$ have discontinuities at the starting and ending points in the phase transition. It is therefore concluded against Ref. [5] that the phase transition is the first order. The same conclusion is also derived in Ref. [10] from a different point of view. It is noted further that the existence of the mixed phase is intrinsic to the first-order phase transition.

Next, we investigate the dependence of liquid-gas phase transition on the asymmetry. Figure 7 shows the pressure-density isotherms for several asymmetries. The dashed curves are spurious results from Eq. (14). The physically realized pressure are the solid curves from Eq. (27). For $a \geq 0.5$ although the dashed curves do not show the nature of van der Waals equation-of-state, the minimization of the Helmholtz energy still leads to the liquid-gas phase transition. The first order phase transition from gas to liquid exists until $a = 0.64$. On the other hands, from $a = 0.65$ to $a = 0.67$ there are upper limits on baryon density, above which we find no solutions of Eqs. (15)-(24) and (27). The absence of phase equilibrium was found first in Ref. [6] and was recovered in the recent work [9]. It was due to the density-dependent [6] or the momentum-dependent [9] effective NN interactions. (Precisely speaking, the treatment of the density dependent ρ-meson coupling in Ref. [6] was not physically accurate because the so-called rearrangement effects [14] were not taken into account.) In the present work it is due to the field-dependent coupling constants (1), which are derived originally from the momentum dependent coupling constants [11] and lead to effective density dependencies. Although there are found in Refs. [6] and [9] the upper limits on pressure, we have the upper limits on baryon density. The difference is because Refs. [6] and [9] investigate the system that is neither canonical nor grand-canonical while we investigate the canonical ensemble. In this respect it is also noted that the discussion on the chemical instability in Refs. [6] and [9] is not applicable to the canonical ensemble in the present work.

From $a = 0.675$ to $a = 0.72$ we see the retrograde condensation. For an example Fig. 8 shows the ratio of liquid as a function of pressure for the asymmetry $a = 0.675$ and the temperature $T = 13$MeV. It decreases steeply after the maximum value is reached. Although the retrograde condensation is discussed in the other works [5,6,8,9], its clear signal, the variation of the ratio of liquid, is presented for the first time in the present paper. Above $a = 0.72$ we have no solutions of Eqs. (15)-(24) and (27) at any baryon density and so the nuclear liquid does not appear.

The above results are summarized in Fig. 9, which shows the section of binodal surface. There is no critical point, on which the liquid branch connects with the gas branch. The gas branch shows a backbend with a bending point at $a = 0.72$, which leads to the retrograde condensation.

We have developed new calculus of the liquid-gas phase transition in the canonical ensemble of asymmetric nuclear matter based on a new RMF model in Refs. [11] and [12]. It is different from the geometrical construction used widely in the other works. The pressure and the chemical potentials are determined for definite values of the baryon densities and the temperature. The pressure increases in the phase transition from gas to liquid against the constant value from the Maxwell construction of the phase equilibrium. The Helmholtz energy is minimized and so is lower than the common tangent. As a result the region of the phase transition is wider than that from the Maxwell construction. The chemical potentials μ_p and μ_n and the derivative of the Gibbs energy $\partial G/\partial P$ have no discontinuities. To the contrary the derivatives of chemical potentials $\partial\mu_p/\partial P$ and $\partial\mu_n/\partial P$ have discontinuities at the ends of the phase transition. We can therefore conclude against the other works that the liquid-gas phase transition in asymmetric nuclear matter is the first order. The liquid and gas branches in the section of binodal surface are connected with each other only on the equal concentration $a = 0$, but there is no critical point. Although the similar result is found using the density-dependent or the momentum-dependent NN interactions, we have confirmed that the absence of the critical point is also reproduced using the field-dependent meson-nucleon coupling constants. Because the gas branch shows a backbend, the retrograde condensation of nuclear liquid has been proved. In a future work we will apply the present calculus to another binary nuclear system, that is, the strange baryon matter.

References

[1] J. Richert and P. Wagner, Phys. Rep. **350** (2001) 1 [arXiv:nucl-th/0009023].

[2] S.D. Gupta, A.Z. Mekjian and M.B. Tsang, *Advances in Nuclear Physics*, Vol. **26** (Kluwer Academic, 2001) [arXiv:nucl-th/0009033].

[3] V.E. Viola *et al.*, Phys. Rep. **434** (2006) 1 [arXiv:nucl-ex/0604012].

[4] V.A. Karnaukhov, Phys. Elem. Part. Atom. Nucl. **37** (2006) 312 [http://www1.jinr.ru/Pepan/Pepan_index.html].

[5] H. Müller and B. D. Serot, Phys. Rev. C **52** (1995) 2072 [arXiv:nucl-th/9505013].

[6] W.L. Qian, R-K. Su and P. Wang, Phys. Lett. B **491** (2000) 90 [arXiv:nucl-th/0008057].

[7] P.K. Panda, G. Klein, D.P. Menezes and C. Providência, Phys. Rev. C **68** (2003) 015201 [arXiv:nucl-th/0306045].

[8] P. Wang, D.B. Leinweber, A.W. Thomas and A.G. Williams, Nucl. Phys. A **748** (2005) 226 [arXiv:nucl-th/0407057].

[9] J. Xu, L-W. Chen, B-A. Li and H-R. Ma, arXiv:nucl-th/0702085.

[10] C. Ducoin, Ph. Chomaz and F. Gulminelli, Nucl. Phys. A **771** (2006) 68 [arXiv:nucl-th/0512029].

[11] K. Miyazaki, Mathematical Physics Preprint Archive (mp_arc) 06-336.

[12] K. Miyazaki, Mathematical Physics Preprint Archive (mp_arc) 07-64.

[13] W.H. Press, S.A. Teukolsky, W.T. Vetterling and B.P. Flannery, Numerical Recipes in C, 2nd edition, 1992, Cambridge University Press [http://www.nr.com/].

[14] F. Hoffman, C.M. Keil and H. Lenske, Phys. Rev. C **64** (2001) 034314.

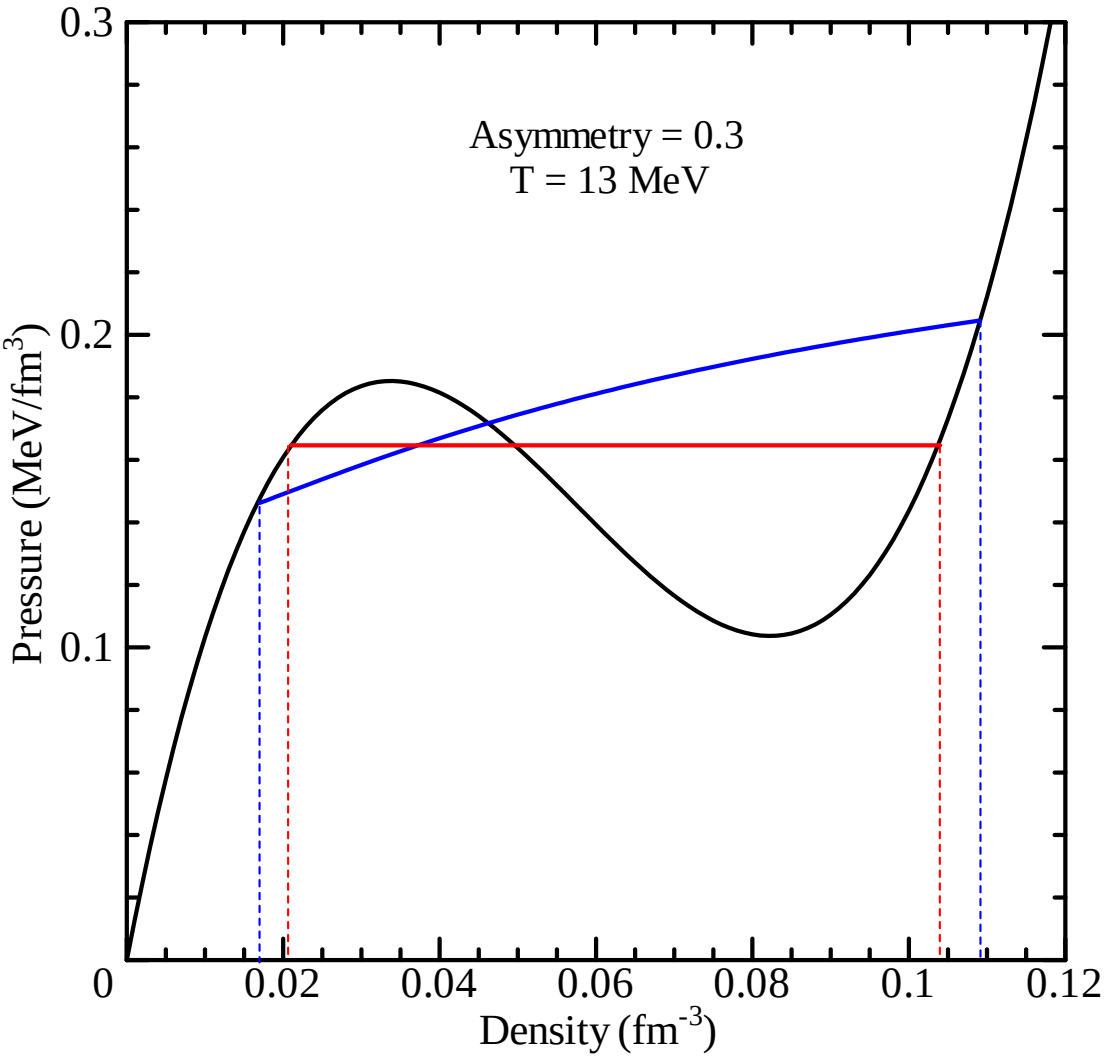

Figure 1: The pressure-density isotherm for the asymmetry $a = 0.3$ and the temperature $T = 13$MeV. The black curve is the result from Eq. (14). The red horizontal line is the pressure in the phase transition derived from the common tangent prescription. The blue curve is the pressure from Eq. (27). The vertical red and blue dashed lines indicate the regions of the phase transition.

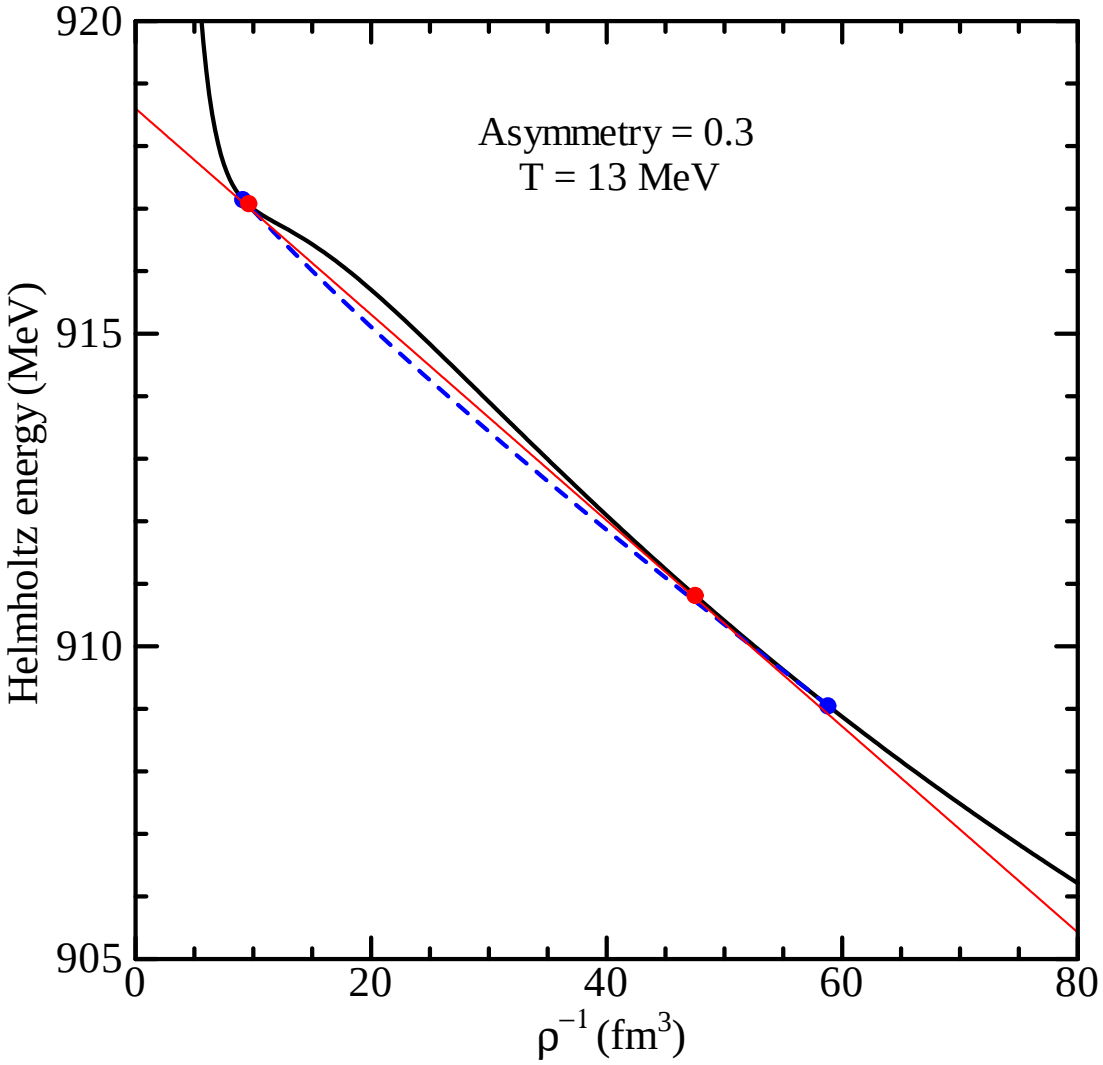

Figure 2: The Helmholtz energy per baryon as a function of volume for the asymmetry $a = 0.3$ and the temperature $T = 13$MeV. The black curve is the result corresponding to the black curve in Fig. 1. The red line is the common tangent that contacts with the black curve on the two red dots. The blue dashed curve between the two blue dots is the minimized Helmholtz energy satisfying the Gibbs condition on the liquid-gas phase equilibrium.

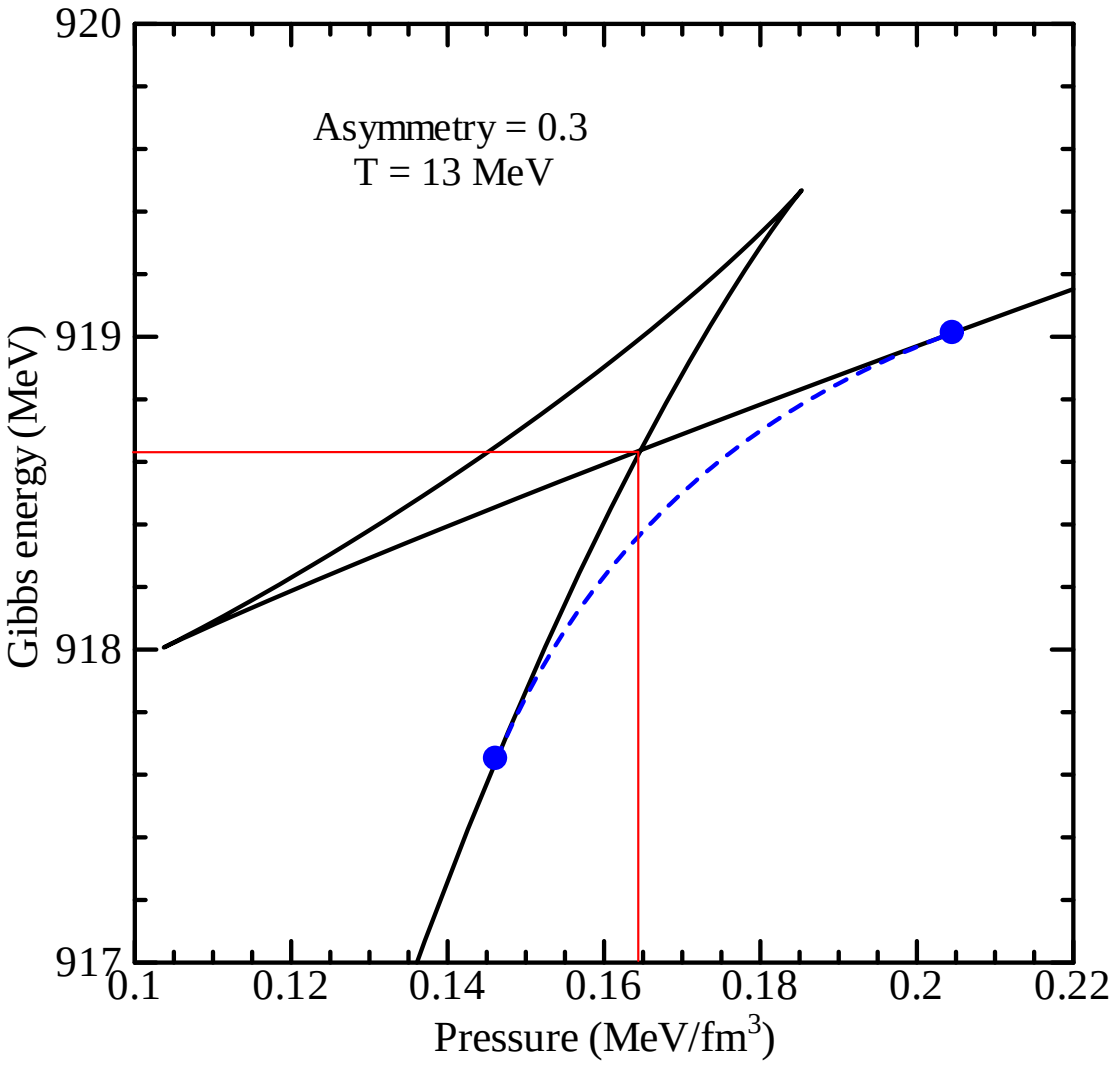

Figure 3: The Gibbs energy per baryon as a function of pressure for the asymmetry $a = 0.3$ and the temperature $T = 13$MeV. The black curve is the result corresponding to the black curve in Fig. 1. It has a crossing point denoted by the red line. The blue dashed curve between the two blue dots is the result satisfying the Gibbs condition on the liquid-gas phase equilibrium.

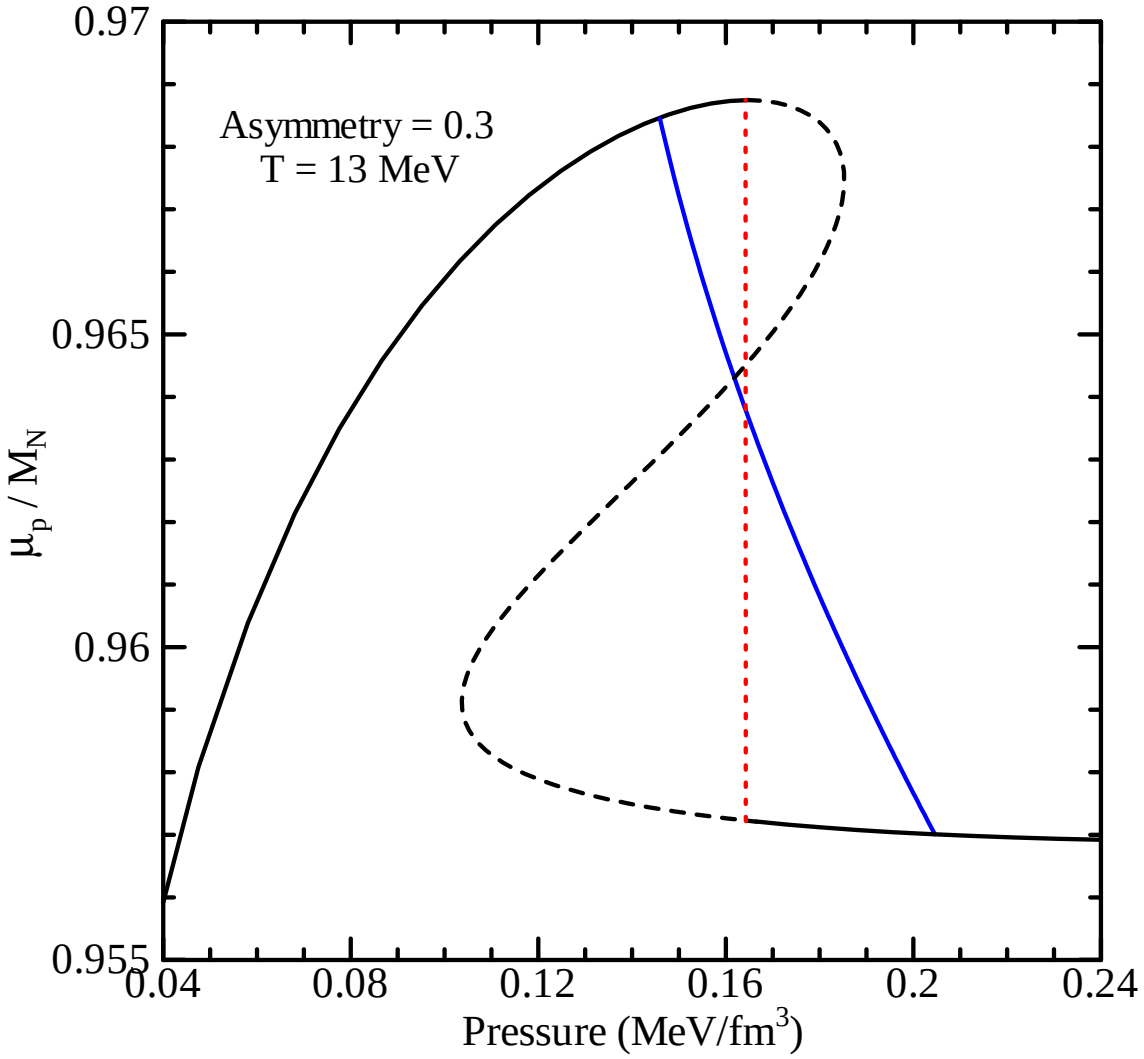

Figure 4: The proton chemical potential as a function of pressure for the asymmetry $a = 0.3$ and the temperature $T = 13$MeV. The black dashed curve corresponds to the concave of the Helmholtz energy in Fig. 2 and so is not realized. Consequently, the black solid curve has a discontinuity denoted by the vertical red dashed line. The blue curve is the result satisfying the Gibbs condition on the liquid-gas phase equilibrium.

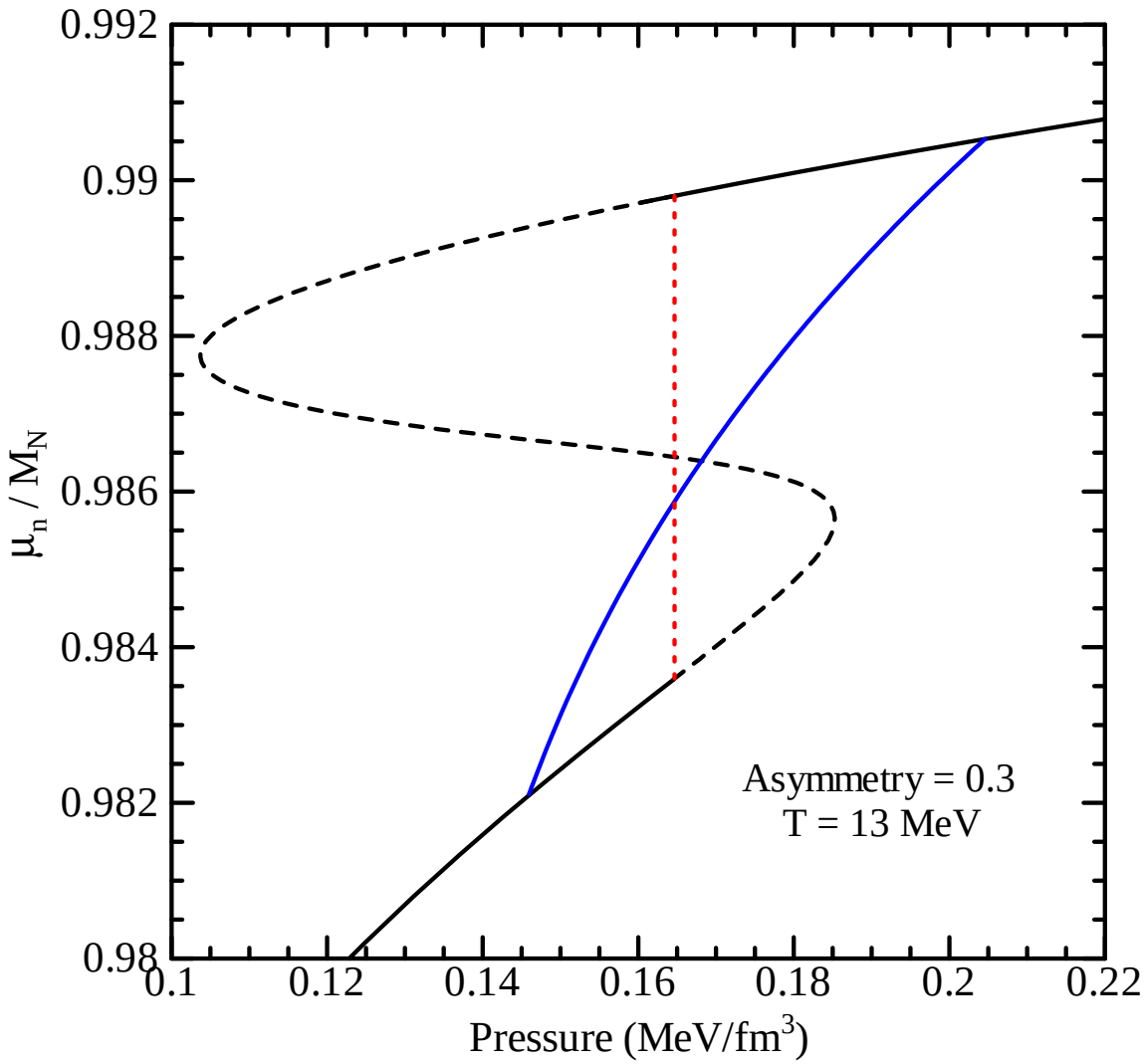

Figure 5: The same as Fig. 4 but for the neutron chemical potential.

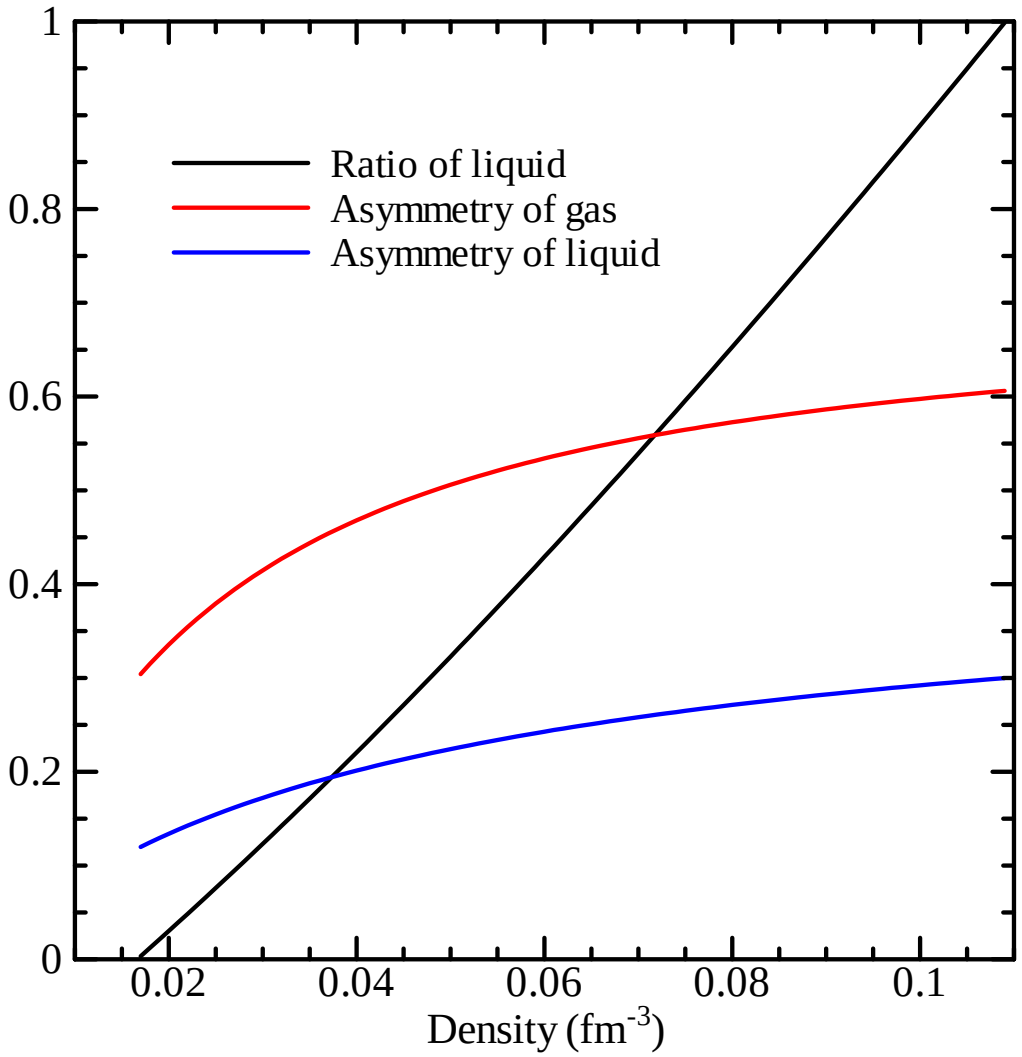

Figure 6: The black curve is the ratio of liquid $f_l = 1 - f_g$ as a function of the baryon density in the phase transition between $\rho_B = 0.017\text{fm}^{-3}$ and 0.109fm^{-3}. The red and blue curves are the asymmetries of gas and liquid, $a_g = \frac{\left(\rho_{Bn}^{(g)} - \rho_{Bp}^{(g)}\right)}{\left(\rho_{Bn}^{(g)} + \rho_{Bp}^{(g)}\right)}$ and $a_l = \frac{\left(\rho_{Bn}^{(l)} - \rho_{Bp}^{(l)}\right)}{\left(\rho_{Bn}^{(l)} + \rho_{Bp}^{(l)}\right)}$.

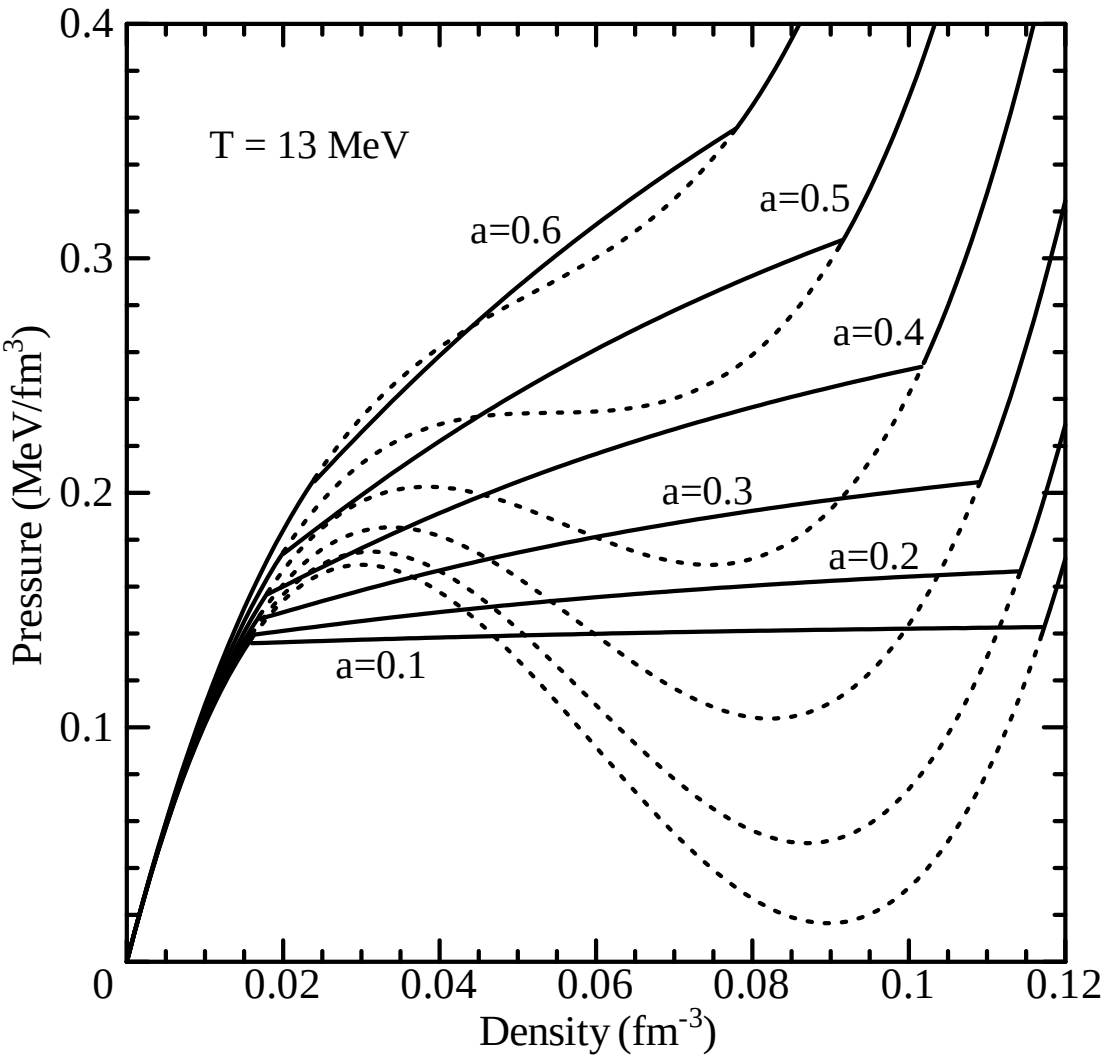

Figure 7: The pressure-density isotherms at $T = 13$MeV for the asymmetries from $a = 0.1$ to $a = 0.6$. The dashed curves from Eq. (14) are spurious while the solid curves from Eq. (27) are realized.

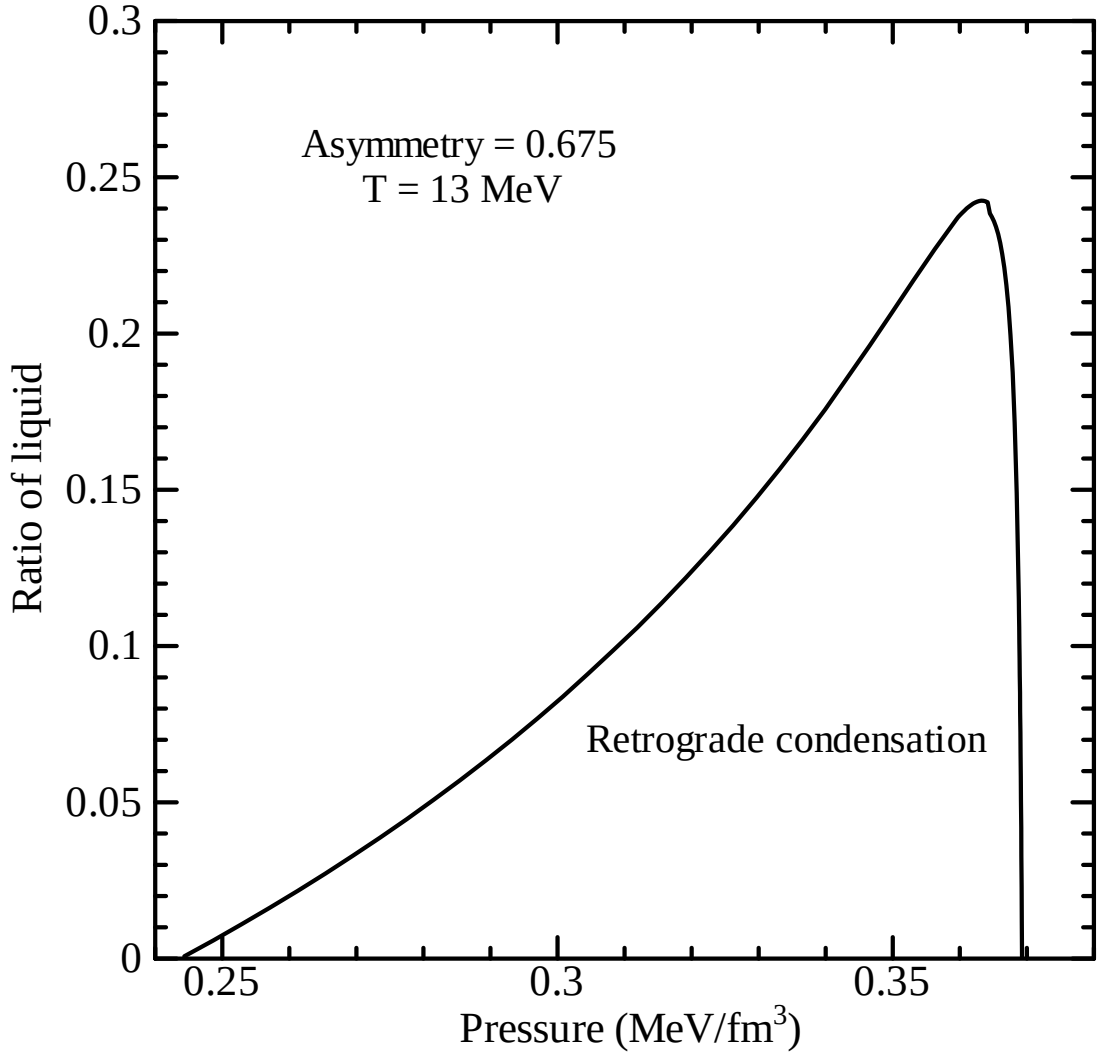

Figure 8: The ratio of liquid as a function of pressure for the asymmetry $a = 0.675$ and the temperature $T = 13$MeV.

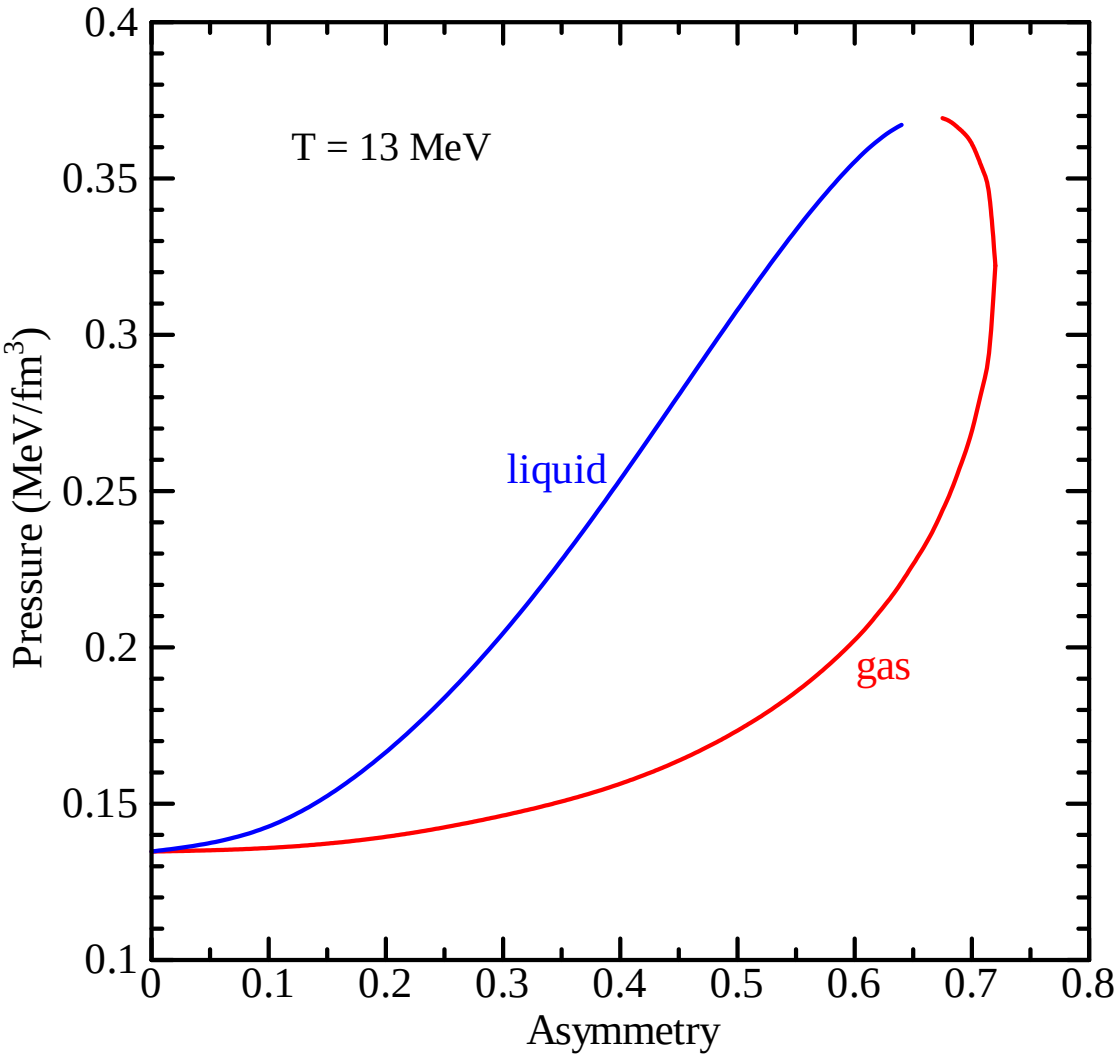

Figure 9: The section of binodal surface at the temperature $T = 13$MeV.